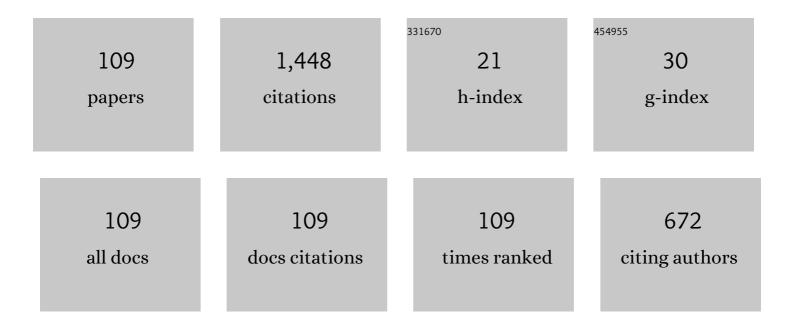
Maogang He

List of Publications by Year in descending order

Source: https://exaly.com/author-pdf/3527482/publications.pdf Version: 2024-02-01



| # | Article | IF | CITATIONS |
|----|---|-----|-----------|
| 1 | Performance comparison of two absorption-compression hybrid refrigeration systems using R1234yf/ionic liquid as working pair. Energy Conversion and Management, 2019, 181, 319-330. | 9.2 | 87 |
| 2 | Vapor–Liquid Equilibrium of R1234yf/[HMIM][Tf ₂ N] and R1234ze(E)/[HMIM][Tf ₂ N] Working Pairs for the Absorption Refrigeration Cycle. Journal of Chemical & Engineering Data, 2016, 61, 3952-3957. | 1.9 | 53 |
| 3 | Vapor–Liquid Equilibrium of Three Hydrofluorocarbons with [HMIM][Tf ₂ N]. Journal of Chemical & Engineering Data, 2015, 60, 1354-1361. | 1.9 | 52 |
| 4 | Investigation on the condensation process of HFO refrigerants by molecular dynamics simulation. Journal of Molecular Liquids, 2019, 288, 111034. | 4.9 | 42 |
| 5 | Solubilities of R-161 and R-143a in 1-Hexyl-3-methylimidazolium bis(trifluoromethylsulfonyl)imide. Fluid Phase Equilibria, 2015, 388, 37-42. | 2.5 | 39 |
| 6 | Vapor-liquid equilibrium and diffusion coefficients of R32 + [HMIM][FEP], R152a + [HMIM][FEP] and R161 + [HMIM][FEP]. Journal of Molecular Liquids, 2018, 253, 28-35. | 4.9 | 35 |
| 7 | Vibrational behavior of single-walled carbon nanotubes based on cylindrical shell model using wave propagation approach. AlP Advances, 2017, 7, . | 1.3 | 33 |
| 8 | Selection and Evaluation of Dry and Isentropic Organic Working Fluids Used in Organic Rankine Cycle Based on the Turning Point on Their Saturated Vapor Curves. Journal of Thermal Science, 2019, 28, 643-658. | 1.9 | 33 |
| 9 | Solubilities of R32, R245fa, R227ea and R236fa in a phosphonium-based ionic liquid. Journal of Molecular Liquids, 2016, 218, 525-530. | 4.9 | 31 |
| 10 | Measurement and correlation of viscosities and densities of methyl dodecanoate and ethyl dodecanoate at elevated pressures. Thermochimica Acta, 2018, 663, 85-92. | 2.7 | 30 |
| 11 | Thermal Diffusivity and Speed of Sound of Saturated Pentane from Light Scattering. International Journal of Thermophysics, 2014, 35, 1450-1464. | 2.1 | 27 |
| 12 | Heat capacities of fatty acid methyl esters from 300 K to 380 K and up to 4.25 MPa. Fuel, 2015, 157, 240-244. | 6.4 | 27 |
| 13 | Diffusion coefficients and Henry's constants of hydrofluorocarbons in [HMIM][Tf 2 N], [HMIM][TfO], and [HMIM][BF 4]. Journal of Chemical Thermodynamics, 2017, 112, 43-51. | 2.0 | 27 |
| 14 | Estimating the viscosity of pure refrigerants and their mixtures by free-volume theory. International Journal of Refrigeration, 2015, 54, 55-66. | 3.4 | 25 |
| 15 | Molecular dynamics simulation of thermophysical properties and condensation process of R1233zd(E). International Journal of Refrigeration, 2020, 112, 341-347. | 3.4 | 25 |
| 16 | Gaseous absorption of fluorinated ethanes by ionic liquids. Fluid Phase Equilibria, 2015, 405, 1-6. | 2.5 | 23 |
| 17 | Viscosity of oxygenated fuel: A model based on Eyring's absolute rate theory. Fuel, 2019, 241, 218-226. | 6.4 | 23 |
| 18 | Measurements and calculations of thermal conductivity for liquid n-octane and n-decane. Fluid Phase Equilibria, 2021, 533, 112940. | 2.5 | 23 |

| # | Article | IF | CITATIONS |
|----|--|-----|-----------|
| 19 | Densities and Viscosities of Ethyl Heptanoate and Ethyl Octanoate at Temperatures from 303 to 353 K and at Pressures up to 15 MPa. Journal of Chemical & Engineering Data, 2017, 62, 2454-2460. | 1.9 | 22 |
| 20 | Solubilities and diffusivities of R227ea, R236fa and R245fa in 1-hexyl-3-methylimidazolium bis(trifluoromethylsulfonyl)imide. Journal of Chemical Thermodynamics, 2018, 123, 158-164. | 2.0 | 22 |
| 21 | Estimating the viscosity of ionic liquid at high pressure using Eyring's absolute rate theory. Fluid Phase Equilibria, 2018, 458, 170-176. | 2.5 | 22 |
| 22 | Experimental and correlational study of isobaric molar heat capacities of fatty acid esters: Ethyl nonanoate and ethyl dodecanoate. Fluid Phase Equilibria, 2019, 479, 47-51. | 2.5 | 22 |
| 23 | Measurement and modeling of thermal conductivity for short chain methyl esters: Methyl butyrate and methyl caproate. Journal of Chemical Thermodynamics, 2021, 159, 106486. | 2.0 | 22 |
| 24 | Improving the viscosity and density of n-butanol as alternative to gasoline by blending with dimethyl carbonate. Fuel, 2021, 286, 119360. | 6.4 | 21 |
| 25 | Isobaric molar heat capacities of 1-ethyl-3-methylimidazolium acetate and 1-hexyl-3-methylimidazolium acetate up to 16ÂMPa. Fluid Phase Equilibria, 2016, 427, 187-193. | 2.5 | 20 |
| 26 | Temperature and pressure dependence of densities and viscosities for binary mixtures of methyl decanoate plus n-heptane. Thermochimica Acta, 2018, 670, 211-218. | 2.7 | 19 |
| 27 | Thermal conductivity measurements for long-chain n-alkanes at evaluated temperature and pressure: n-dodecane and n-tetradecane. Journal of Chemical Thermodynamics, 2021, 162, 106566. | 2.0 | 18 |
| 28 | Solubilities of small hydrocarbons, viscosities of diluted tetraalkylphosphonium bis(2,4,4â€ŧrimethylpentyl) phosphinates. AICHE Journal, 2014, 60, 2607-2612. | 3.6 | 17 |
| 29 | Isobaric heat capacities of ethyl heptanoate and ethyl cinnamate at pressures up to 16.3 MPa. Journal of Chemical Thermodynamics, 2016, 93, 70-74. | 2.0 | 17 |
| 30 | Prediction of Thermal Conductivity for Guiding Molecular Design of Liquids. ACS Sustainable Chemistry and Engineering, 2020, 8, 6022-6032. | 6.7 | 17 |
| 31 | Effects of Liquid Supply Method on Falling-Film Mode Transitions on Horizontal Tubes. Heat Transfer Engineering, 2013, 34, 562-579. | 1.9 | 16 |
| 32 | Measurement of isobaric heat capacity of pure water up to supercritical conditions. Journal of Supercritical Fluids, 2015, 100, 1-6. | 3.2 | 16 |
| 33 | Speed of Sound in Methyl Caprate, Methyl Laurate, and Methyl Myristate: Measurement by Brillouin Light Scattering and Prediction by Wada's Group Contribution Method. Energy & Fuels, 2016, 30, 9502-9509. | 5.1 | 16 |
| 34 | Isobaric molar heat capacities of binary mixtures containing methyl caprate and methyl laurate at pressures up to 16.2 MPa. Thermochimica Acta, 2017, 651, 43-46. | 2.7 | 16 |
| 35 | Prediction of the critical properties of mixtures based on group contribution theory. Journal of Molecular Liquids, 2018, 271, 313-318. | 4.9 | 16 |
| 36 | Surface Tension of Aqueous Solutions of Small-Chain Amino and Organic Acids. Journal of Chemical & Engineering Data, 2019, 64, 5049-5056. | 1.9 | 16 |

| # | Article | IF | CITATIONS |
|----|---|-----|-----------|
| 37 | Heat Capacities of Fluids: The Performance of Various Equations of State. Journal of Chemical & Engineering Data, 2020, 65, 5654-5676. | 1.9 | 16 |
| 38 | Mass Diffusion Coefficients of Dimethyl Carbonate in Heptane and in Air at <i>T</i> = (278.15 to 338.15) K. Journal of Chemical & Engineering Data, 2008, 53, 2861-2864. | 1.9 | 15 |
| 39 | Unusual Transformation of Polymer Coils in a Mixed Solvent Close to the Critical Point. Physical Review Letters, 2018, 121, 207802. | 7.8 | 15 |
| 40 | Isobaric molar heat capacities measurement of binary mixtures containing ethyl laurate and ethanol at high pressures. Journal of Molecular Liquids, 2019, 280, 301-306. | 4.9 | 15 |
| 41 | Absorption and separation of CO2/C3H8 and C3H6/C3H8 by ionic liquid: Effect of molar volume. Journal of Natural Gas Science and Engineering, 2018, 58, 266-274. | 4.4 | 14 |
| 42 | Isobaric Molar Heat Capacity of Ethyl Octanoate and Ethyl Decanoate at Pressures up to 24 MPa. Journal of Chemical & Engineering Data, 2018, 63, 2252-2256. | 1.9 | 14 |
| 43 | Determination of Binary Gas Diffusion Coefficients Using Digital Holographic Interferometry. Journal of Chemical & Engineering Data, 2010, 55, 3318-3321. | 1.9 | 13 |
| 44 | Measurement of the Speed of Sound in Hexane and Heptane at Temperatures from (303.15 to 536.15) K and Pressures from (1.0 to 8.5) MPa. Journal of Chemical & Engineering Data, 2016, 61, 701-711. | 1.9 | 13 |
| 45 | Correlation for viscosities of pure liquids at high pressures. Journal of Molecular Liquids, 2017, 231, 404-410. | 4.9 | 13 |
| 46 | Quantification of Dipolar Contribution and Modeling of Green Polar Fluids with the Polar Cubic-Plus-Association Equation of State. ACS Sustainable Chemistry and Engineering, 2021, 9, 7602-7619. | 6.7 | 13 |
| 47 | Regulating structure and flow of ionic liquid confined in nanochannel using water and electric field. Journal of Molecular Liquids, 2022, 351, 118612. | 4.9 | 13 |
| 48 | Thermal conductivity analysis of two-dimensional complex plasma liquids and crystals. Physics of Plasmas, 2020, 27, . | 1.9 | 12 |
| 49 | Modeling heat capacity of saturated hydrocarbon in liquid phase over a wide range of temperature and pressure. Journal of Molecular Liquids, 2020, 319, 114068. | 4.9 | 12 |
| 50 | General models for prediction densities and viscosities of saturated and unsaturated fatty acid esters. Journal of Molecular Liquids, 2021, 341, 117374. | 4.9 | 12 |
| 51 | Experimental Studies of Thermal Conductivity of Three Biodiesel Compounds: Methyl Pentanoate, Methyl Octanoate, and Methyl Decanoate. Journal of Chemical & Engineering Data, 2022, 67, 45-53. | 1.9 | 12 |
| 52 | Experimental investigation and modeling of thermophysical properties of ethyl decanoate at high temperatures. Fluid Phase Equilibria, 2019, 501, 112274. | 2.5 | 11 |
| 53 | Experimental Study on Isobaric Molar Heat Capacities of a Deep Eutectic Solvent: Choline Chloride + Ethylene Glycol. Journal of Chemical & Engineering Data, 2020, 65, 690-695. | 1.9 | 11 |
| 54 | Measurement of the thermal conductivity of the components of biodiesels: Methyl laurate and methyl myristate. Fluid Phase Equilibria, 2022, 556, 113409. | 2.5 | 11 |

| # | Article | IF | CITATIONS |
|----|---|-----|-----------|
| 55 | Isobaric Heat Capacity of Boric Acid Solution. Journal of Chemical & Engineering Data, 2014, 59, 4200-4204. | 1.9 | 10 |
| 56 | Mutual diffusion coefficients of ethanolÂ+Ân-heptane and diethyl carbonateÂ+Ân-heptane from 288.15ÂK to 318.15ÂK. Journal of Chemical Thermodynamics, 2020, 144, 106089. | 2.0 | 10 |
| 57 | Measurement of critical properties for binary and ternary mixtures containing potential gasoline additive diethyl carbonate (DEC). Fluid Phase Equilibria, 2018, 471, 17-23. | 2.5 | 9 |
| 58 | Gaseous Absorption of <i>trans</i> -1-Chloro-3,3,3-trifluoropropene in Three Immidazolium-Based Ionic Liquids. Journal of Chemical & Engineering Data, 2018, 63, 1780-1788. | 1.9 | 9 |
| 59 | Mesoscopic Diffusion of Poly(ethylene oxide) in Pure and Mixed Solvents. Journal of Physical Chemistry B, 2018, 122, 3454-3464. | 2.6 | 9 |
| 60 | First law-based thermodynamic analysis on Kalina cycle. Frontiers of Energy and Power Engineering in China, 2008, 2, 145-151. | 0.4 | 8 |
| 61 | A New Method of Processing Mach–Zehnder Interference Fringe Data in Determination of Diffusion Coefficient. International Journal of Thermophysics, 2009, 30, 1823-1837. | 2.1 | 8 |
| 62 | Mutual diffusion behavior of short chain alcohols+n-octane mixtures. Thermochimica Acta, 2016, 624, 1-7. | 2.7 | 8 |
| 63 | A new power/cooling cogeneration system using R1234ze(E)/ionic liquid working fluid. International Journal of Energy Research, 2020, 44, 4703-4716. | 4.5 | 8 |
| 64 | Fouling formed on SS316L tube surface from thermal oxidative degradation of exo -tetrahydrodicyclopentadiene. Applied Thermal Engineering, 2017, 118, 464-470. | 6.0 | 7 |
| 65 | A Comprehensive Study on Thermophysical Properties of Carbon Dioxide through the Cubic-Plus-Association and Crossover Cubic-Plus-Association Equations of State. Journal of Chemical & Engineering Data, 2020, 65, 4268-4284. | 1.9 | 7 |
| 66 | Ultra-accurate thermophysical properties of helium-4 and helium-3 at low density. I. Second pressure and acoustic virial coefficients. Molecular Physics, 2021, 119, e1802525. | 1.7 | 7 |
| 67 | Unique Arrangement of Atoms Leads to Low Thermal Conductivity: A Comparative Study of Monolayer Mg ₂ C. Journal of Physical Chemistry Letters, 2021, 12, 10353-10358. | 4.6 | 7 |
| 68 | Measurement of the Speed of Sound in Near-Critical and Supercritical <i>n</i> -Heptane at Temperatures from (513.40 to 650.90) K and Pressures from (2.5 to 10.0) MPa. Journal of Chemical & Engineering Data, 2018, 63, 3331-3337. | 1.9 | 6 |
| 69 | Speed of Sound and Derived Properties of Ethyl Nonanoate. Journal of Chemical & Engineering Data, 2019, 64, 3632-3640. | 1.9 | 6 |
| 70 | Thermodynamic and Economic Studies of a Combined Cycle for Waste Heat Recovery of Marine Diesel Engine. Journal of Thermal Science, 2022, 31, 417-435. | 1.9 | 6 |
| 71 | Development status and some considerations on Energy Internet construction in Beijing-Tianjin-Hebei region. Heliyon, 2022, 8, e08722. | 3.2 | 6 |
| 72 | Thermodynamic optimization of lithium chloride-potassium chloride-zinc chloride and lithium chloride-potassium chloride-magnesium chloride for thermal energy storage. Journal of Energy Storage, 2022, 53, 105028. | 8.1 | 6 |

| # | Article | IF | CITATIONS |
|----|---|-----|-----------|
| 73 | Data-driven multi-objective molecular design of ionic liquid with high generation efficiency on small dataset. Materials and Design, 2022, 220, 110888. | 7.0 | 6 |

Mutual Diffusion Coefficients of Diethyl Carbonate and Diethyl Adipate in Heptane at T = (278.15 to) Tj ETQq0 0 0 rgBT /Overlock 10 Tf

| 75 | Measurements of the Speed of Sound in Liquid and Supercritical <i>n</i> -Octane and Isooctane. Journal of Chemical & Engineering Data, 2018, 63, 102-112. | 1.9 | 5 |
|----|---|-----|---|
| 76 | Densities and Viscosities of Mixtures of Methyl Dodecanoate + Ethyl Octanoate at Pressures up to 15 MPa. Journal of Chemical & Engineering Data, 2018, 63, 4085-4094. | 1.9 | 5 |
| 77 | Measurement of Critical Properties for Binary and Ternary Mixtures Containing n-Butanol and n-Alkane. Journal of Chemical & Engineering Data, 2018, 63, 3956-3965. | 1.9 | 5 |
| 78 | Measurement of thermal diffusivity for carbon dioxide (CO2) at TÂ= 293.15–406.15â€ [–] K and pressures up to 11â€ [–] MPa by dynamic light scattering (DLS). Fluid Phase Equilibria, 2018, 474, 126-130. | 2.5 | 5 |
| 79 | Isothermal titration calorimetry in a 3D-printed microdevice. Biomedical Microdevices, 2019, 21, 96. | 2.8 | 5 |
| 80 | General Model Based on Artificial Neural Networks for Estimating the Viscosities of Oxygenated Fuels. ACS Omega, 2019, 4, 16564-16571. | 3.5 | 5 |
| 81 | A new activity coefficient model for the solution of molecular soluteÂ+Âionic liquid. Fluid Phase Equilibria, 2019, 493, 144-152. | 2.5 | 5 |
| 82 | Measurement of critical temperature and critical pressure of tert-butanol and alkane mixtures. Journal of Molecular Liquids, 2020, 302, 112582. | 4.9 | 5 |
| 83 | Experimental measurement and prediction of thermal conductivity of fatty acid ethyl esters: ethyl butyrate and ethyl caproate. Fluid Phase Equilibria, 2022, 560, 113507. | 2.5 | 5 |
| 84 | Thermal Diffusivity of 2-Ethoxy-2-methylpropane (ETBE) and 2-Methoxy-2-methylbutane (TAME) at Temperatures from (293 to 523) K and Pressure up to 10 MPa. Journal of Chemical & Engineering Data, 2017, 62, 893-901. | 1.9 | 4 |
| 85 | Two-Binary-Interaction-Parameter Model for Molecular Solute + Ionic Liquid Solution. Industrial & Engineering Chemistry Research, 2021, 60, 11490-11501. | 3.7 | 4 |
| 86 | Two Crossover Soave–Redlich–Kwong Equations of State with Fully Analytical Crossover Functions for the Thermodynamic Properties of Carbon Dioxide. Industrial & Engineering Chemistry Research, 2021, 60, 15301-15309. | 3.7 | 4 |
| 87 | Tuning the Molecular Structure and Transport Property of [bmim][Tf2N] Using Electric Field. Journal of Thermal Science, 2022, 31, 1076-1083. | 1.9 | 4 |
| 88 | lsobaric heat capacities of exo-tetrahydrodicyclopentadiene at temperatures from 323ÂK to 523ÂK and pressures up to 6ÂMPa. Fluid Phase Equilibria, 2017, 434, 102-106. | 2.5 | 3 |
| 89 | Measurement and Correlation of the Solubilities of Oxygen, Nitrogen, and Carbon Dioxide in JP-10. Journal of Chemical & Engineering Data, 2017, 62, 3998-4005. | 1.9 | 3 |
| 90 | Speed of Sound and Derivative Properties of Ethyl Laurate from Rayleigh–Brillouin Light-Scattering Spectroscopy. Journal of Chemical & Engineering Data, 2020, 65, 3146-3160. | 1.9 | 3 |

| # | Article | IF | CITATIONS |
|-----|--|-----|-----------|
| 91 | Speed of sound for ethanol in vicinity of the critical point from Rayleigh-Brillouin light scattering spectroscopy. Fluid Phase Equilibria, 2020, 515, 112585. | 2.5 | 3 |
| 92 | Speed of sound measurement and mixing-rule evaluation of (n-butanolÂ+Ân-heptane) binary mixtures. Journal of Chemical Thermodynamics, 2022, 172, 106817. | 2.0 | 3 |
| 93 | Measurement of the speed of sound in supercritical n–hexane at temperatures from (509.17–637.99) K and pressures from (3.5–7.5) MPa. Fluid Phase Equilibria, 2019, 497, 97-103. | 2.5 | 2 |
| 94 | Speed of Sound Measurement in 1-Methoxy-2-propanol from (306.81 to 648.29) K and up to 10 MPa. Journal of Chemical & Engineering Data, 2019, 64, 337-344. | 1.9 | 2 |
| 95 | Measurement of the speed of sound in n-decane at temperatures from (298.32 to 653.95) K and pressures up to 10.0ÂMPa. Journal of Chemical Thermodynamics, 2020, 148, 106127. | 2.0 | 2 |
| 96 | Numerical Study of Flow and Heat Transfer in a Rectangular Channel Partially Filled with Porous Media at the Pore Scale Using Lattice Boltzmann Method. Heat Transfer Engineering, 2022, 43, 818-829. | 1.9 | 2 |
| 97 | Association effect on the density, viscosity and excess properties of fatty acid esterÂ+Âalcohol mixtures: Experiment and modeling. Fuel, 2022, 316, 123425. | 6.4 | 2 |
| 98 | Isobaric Molar Heat Capacities of Binary Mixtures of Diethyl Carbonate and Methyl Caprate at High Pressures. Journal of Chemical & Engineering Data, 2022, 67, 661-668. | 1.9 | 2 |
| 99 | Speed of Sound Measurements of 2-Methoxy-2-methylpropane in the Temperature Range of 293.15 and 673.15 K and for Pressures up to 10 MPa. Journal of Chemical & Engineering Data, 2016, 61, 3127-3134. | 1.9 | 1 |
| 100 | Measurement of the Speed of Sound in Methyl Caprylate from 298.22 to 608.38 K and up to 10 MPa. Journal of Chemical & Engineering Data, 2019, 64, 3617-3623. | 1.9 | 1 |
| 101 | Thermo-Acoustic Properties of (Ethanol + <i>n</i> -Heptane) Binary Mixtures from 293.35 to 433.89 K and up to 5.0 MPa. Journal of Chemical & Engineering Data, 2020, 65, 3893-3905. | 1.9 | 1 |
| 102 | Measurement of Thermal Diffusivity of n-Pentane from (293–573) K and up to 10.0 MPa in the Near-Critical and Supercritical Regions. Journal of Chemical & Engineering Data, 0, , . | 1.9 | 1 |
| 103 | Measurement of the critical temperature and critical pressure of isopropanol and isobutanol blended with gasoline components. Journal of Supercritical Fluids, 2022, 182, 105536. | 3.2 | 1 |
| 104 | Measurement of the speed of sound in near-critical n-dodecane at temperatures from (433 to 679) K and pressures up to 10.0ÂMPa. Journal of Chemical Thermodynamics, 2022, 170, 106768. | 2.0 | 1 |
| 105 | Speed of Sound and Excess Properties of (Ethanol + Isooctane) Binary System. Journal of Chemical & Engineering Data, 2022, 67, 1428-1437. | 1.9 | 1 |
| 106 | Measurement of Speed of Sound in Methyl Hexanoate from 297.83 to 588.07 K and up to 10 MPa. Journal of Chemical & Engineering Data, 2019, 64, 5698-5704. | 1.9 | 0 |
| 107 | Measurement of the speed of sound in supercritical n-pentane at temperatures from (422.69–653.53) K and pressures from (3.5–10.0) MPa. Fluid Phase Equilibria, 2020, 507, 112390. | 2.5 | 0 |
| 108 | Dynamic motions and architectural changes in DNA supramolecular aggregates visualized via transmission electron microscopy without liquid cells. Nanoscale, 2021, 13, 15928-15936. | 5.6 | 0 |

| # | Article | IF | CITATIONS |
|-----|--|-----|-----------|
| 109 | Isobaric molar heat capacities of dimethyl carbonate and alkane binary mixtures at high pressures. Journal of Thermal Analysis and Calorimetry, 0, , 1. | 3.6 | 0 |